



## THERMAL AND MECHANICAL PROPERTIES OF AN IRON BASED AMORPHOUS ALLOY

\*M. IQBAL and W.H. WANG<sup>1</sup>

Microstructural Studies Group, Physics Division, PINSTECH, P.O. Nilore, Islamabad, Pakistan

<sup>1</sup>Institute of Physics, Chinese Academy of Sciences, Beijing, China

(Received March 31, 2014 and accepted in revised form May 27, 2014)

The Fe-Si-B is a well known system of technical importance used for various applications due to promising magnetic properties and corrosion resistant. Melt spun ribbons (MSRs) of 50  $\mu\text{m}$  thickness of  $\text{Fe}_{77.5}\text{Si}_{13.3}\text{B}_{9.2}$  alloy were produced by melt spinning technique. Master alloys were prepared by using 3-4 N pure metals. The alloy was characterized by X-ray diffraction (XRD), differential scanning calorimetry (DSC), stereo scan and scanning electron microscopy (SEM) techniques. Elemental analysis was conducted by energy dispersive X-ray analyzer (EDAX). DSC results confirmed that the alloy showed wide supercooled liquid region before crystallization indicating good thermal stability. Activation energy was calculated to be 397 kJ/mol. Vicker's and nanohardness as well as elastic modulus were measured. Nanohardness (H) to elastic modulus (E) ratio (H/E) indicates existence of covalent bonding in Fe-B-Si amorphous alloy. It is expected that the alloy is fit for fabrication of small electronics components, jewelry applications, structural materials and core windings of "Green transformers".

**Keywords:** Fe-based alloys, Mechanical properties, Thermal properties, Activation energy, Nanohardness, Elastic modulus

### 1. Introduction

It is well established that amorphous alloys have better physical, mechanical and thermal properties as compared to their crystalline counterparts due to their random and non-equilibrium structure. Fe-based alloys have wide range of applications [1-3] as they have unique magnetic properties and can be used as ferromagnetic and paramagnetic materials [4-5] depending upon the solute elements used with the solvent. There is a unique complete Surat in Chapter 27 of the Holy Book "Al-Quran" named as "Al-Hadid (The Iron)" verse number 25, God stated as "And We sent down iron, wherein is great military might and benefits for the people". The history of making Fe-based alloys is thousands years old. In Surat Kahaf, verse numbers 96-97, Chapters 15-16 of Al-Quran, it is stated "Bring me sheets of iron until, when he had leveled (them) between the two mountain walls, he said, "Blow (with bellows), until when he had made it (like) fire, he said, "Bring me, that I may pour over it molten copper." So Gog and Magog were unable to pass over it, nor were they able (to effect) in it any penetration". See and consult website (Quran.com) for reference. Fe-based alloys are also used for decolorization of azo dyes [6-8] as well as for core windings of "Amorphous green transformers" [9-12]. Replacement of Si steel used in electric transformers by amorphous Fe-B-Si melt spun ribbons is growing in Asia especially in China, Japan and India due to extraordinary benefits. This trend is also growing in America and Europe as Fe-based

amorphous alloys are relatively cheap, easily available and have excellent magnetic properties. Although Fe-B-Si system has widely studied [13-16] but there is no report available on this system about its elastic recovery and bonding nature. The enthalpies of mixings of Fe-B, Fe-Si and B-Si pairs are -26, -35 and -14 kJ/mol respectively. The atomic sizes of Fe, Si and B atoms are 0.12412, 0.11530 and 0.08200 nanometers (nm) respectively. Small size atoms such as B, C and Si are added in Fe to enhance the atomic packing density which affects the properties of the base material. In this manuscript, the results on Vicker's and nanohardness, elastic modulus, thermal properties and activation energy are presented.

### 2. Experimental

Melt spun ribbons (MSRs) of about 50  $\mu\text{m}$  thickness of  $\text{Fe}_{77.5}\text{Si}_{13.3}\text{B}_{9.2}$  alloy were produced by melt spinning technique. Alloy buttons were prepared by using 3-4N pure metals of Fe, Si and Fe-B master alloy by melting the alloy mixture in arc melting furnace at least four times to get the extended chemical homogeneity. MSRs were produced under inert (using 5N pure Ar) atmosphere to avoid oxidation. Thermal behavior of the alloy was studied by low and high temperature differential scanning calorimetry (DSC) employing Perkin Elmer 7/Pyris DSC and NETZSCH DSC 404 F3 systems. Structural studies of the materials produced were done by X-ray diffraction (XRD) RIGAKU

\* Corresponding author : miqbalchishti@gmail.com

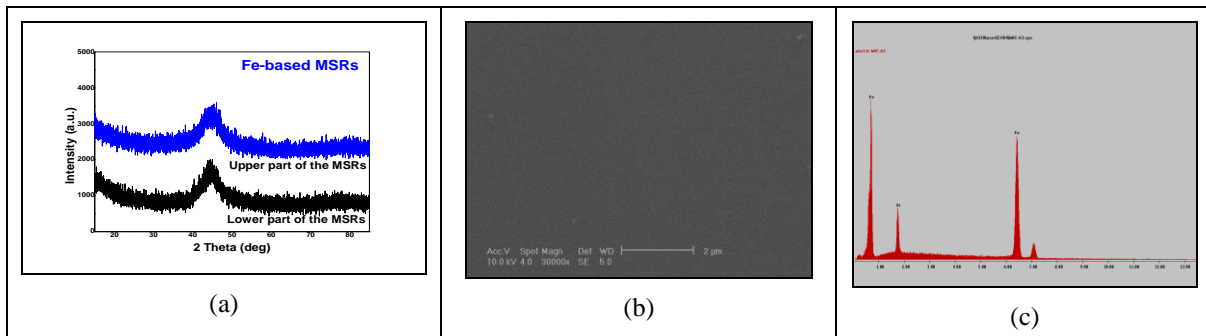


Figure 1 (a) XRD patterns of upper and lower surfaces of MSR, (b) featureless surface of the as cast material and (c) EDS spectrum of the alloy showing Fe & Si and a small B peak.

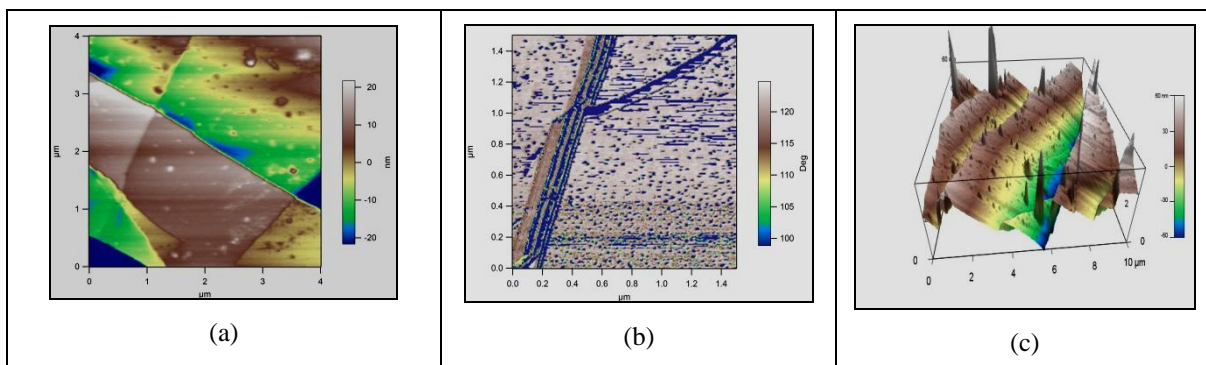


Figure 2 (a, b). Viewgraphs taken by AFM showing intersected shear bands and (c) second phase particles over the surface in cut pieces of as cast MSR.

Diffractometer using  $\text{Cu K}\alpha_1$  radiation (wavelength  $\lambda = 1.54056 \text{ \AA}$ ). Selected samples of MSR were observed by stereo scan microscope, scanning electron microscope (SEM LEO 440i) and atomic force microscope (AFM). Samples were analyzed by energy dispersive X-ray analyzer (EDAX) Oxford Link (ISIS 300). Vicker's microhardness was measured by "Everone hardness tester" under an appropriate load of 100-200 gmf. Nanohardness was measured by using "MTS Nanohardness tester" under an appropriate load. Nanohardness (H) to elastic modulus (E) ratio (H/E) was calculated.

### 3. Results and Discussion

XRD patterns of both sides of as cast MSR of the  $\text{Fe}_{77.5}\text{Si}_{13.3}\text{B}_{9.2}$  alloy are shown in Figure 1(a). The broad bands without any appreciable diffraction peaks confirmed the amorphous nature of the materials produced. SEM examination shows featureless surface of the MSR as shown in Figure 1(b) for the alloy. The MSR prepared have the excellent metallic luster. No defects (such as voids, pores or any precipitates) in the material were observed. The EDAX spectrum of the matrix is shown in Figure 1(c). Fe and Si peaks are very strong as those are in high concentrations. As light

elements such as Boron can't exactly detected by EDAX, even then, a small peak of boron is visible in the spectrum. Cut pieces of as cast MSR (cut by pair of scissors) were observed by AMF showing that samples aren't smooth and show sample roughness. Shear bands and second phase particles in various areas over the rough surface were observed in cut pieces of MSR as shown in Figure 2(a) and Figure 2(b). The particles shown in Figure 2(c) were checked by EDAX and analysis shows high oxygen content at the sample surface in addition to Fe and Si. Second phase particles and zones containing precipitates are found to be rich in Fe and O as confirmed by electron probe micro analysis.

Low and high temperature DSC was conducted at various heating rates "r". High temperature DSC scan at 10 K/min is shown in Figure 3(a). Exothermic and endothermic reactions are clear and a number of thermal parameters are evaluated. Thermal parameters like glass transition temperature  $T_g$ , crystallization temperature  $T_x$ , peak temperature  $T_p$ , melting temperature  $T_m$  and liquidus temperature  $T_l$ , a fundamental key parameter usually called "reduced glass transition temperature"  $T_{rg1} (= T_g/T_m \text{ and } T_{rg2} = T_g/T_l)$ ,  $\gamma = T_x/(T_l+T_g)$  [17],

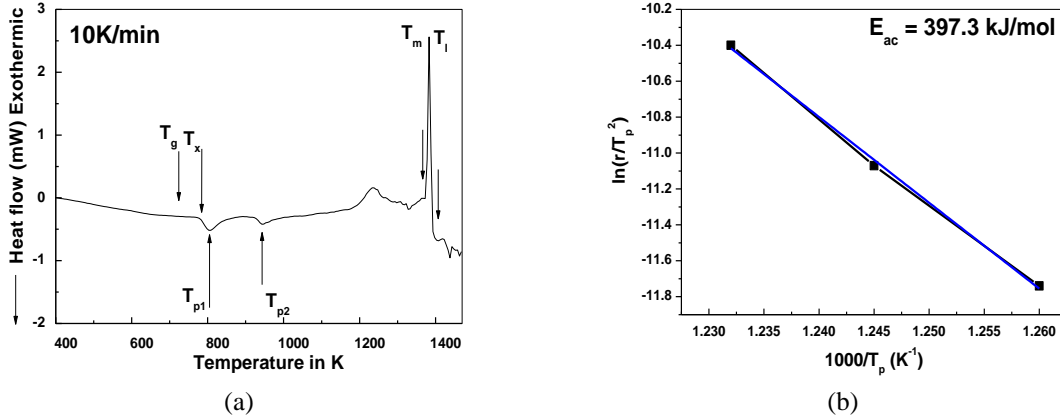


Figure 3 (a). High temperature DSC of the alloy at 10 K/min and (b) Kissinger plot for calculation of activation energy.

Table 1. Thermal parameter (in K) deduced for the alloy at heating rate of 10 K/min

$T_g$	$T_x$	$\Delta T_x$	$T_{p1}$	$T_{p2}$	$T_m$	$T_l$	$\gamma$	$\beta$	$\delta$
724	784	60	806	943	1372	1393	0.37	1.53	1.17
$\omega$	$K_H$	$K_W$	$K_{LL}$	$K_{SP}$	$K_1$	$K_2$	$K_3$	$K_4$	$E_{ac}$ (kJ/mol)
0.24	0.10	0.044	0.374	1.823	648	60	0.57	0.962	397.3

$\delta = T_x/(T_l - T_g)$  [18],  $\beta = T_g \cdot T_x / (T_l - T_x)^2$  [19] and  $\omega = T_g/T_x - 2T_g/(T_g + T_l)$  [20] are calculated. The results are presented in Table 1. Some more thermal parameters such as Hruby parameter  $K_H = \Delta T_x / (T_m - T_x)$  [21], thermal parameter proposed by Saad and Poulain  $K_{SP} = (T_p - T_x)(\Delta T_x / T_g)$  [22], Weinberg parameter  $K_W = \Delta T_x / T_m$ ,  $K_{LL} = T_x / (T_g + T_m)$  [23],  $K_1 = T_m - T_g$ ,  $K_2 = \Delta T_x$ ,  $K_3 = T_x / T_m$  and  $K_4 = (T_p - T_x)(\Delta T_x / T_m)$  [24] are calculated and given in Table 1. The alloy produced has high melting ( $T_m$ ) and liquidus ( $T_l$ ) temperatures. The comparison of relative ratios of basic parameters such as  $T_{rg}$ ,  $\gamma$ ,  $\delta$ ,  $\beta$  and  $\omega$  show good thermal properties. These thermal parameters show complete thermal behavior while width of supercooled liquid region ( $\Delta T_x$ ) shows good thermal stability of the alloy as confirmed by calculation of activation energy. Supercooled liquid region and value of  $\gamma$  was obtained about 60 K and 0.37 which is similar to  $Fe_{76}P_5[Si_{0.3}B_{0.5}Co_{0.2}]_{19}$  alloy [25]. The dependency of crystallization temperature on heating rate was used to determine the associated activation energy ( $E_{ac}$ ) by means of Kissinger's equation  $\ln(r/T_p^2) = -E_{ac}/RT_p + \text{constant}$ . Here "r" stands for the heating rate,  $T_p$  is the peak temperature in DSC scans, R is the gas constant 8.3145 J/mol K, with slope  $-E_{ac}/R = B$ , where B is a constant [26]. Activation energy was calculated by Kissinger plot shown in Figure 3(b) and found to be 397.3 kJ/mol. It shows high resistance of the

alloy against crystallization and reconfirms the high thermal stability of the alloy.

Hardness is a measure of a material's resistance to plastic deformation. Vicker's hardness  $H_V$ , nanohardness H (GPa) and elastic modulus (GPa) of as cast MSRs was measured and found to be 760, 11.2 GPa and 170 GPa respectively. These values are higher than many ferrous and nonferrous alloys indicating good mechanical properties. The promising mechanical properties are due to enhanced closed packed density by introducing small size Boron (B) atoms in between Fe and Si atoms in amorphous matrix of iron. Vicker's and three sided Berkovich indents for the alloy are shown in Figure 4(a) and Figure 4(b) respectively. Semicircular shear bands and vertical cracks around the Vicker's indents were observed as clear in Figure 4(a). It shows that the base material is brittle but a little plasticity exists. Therefore these MSRs can easily be cut down. On the other hand, Berkovich indents don't show any slip bands around the indents. The reason is that tip of the nanoindenter penetrate in steps slowly under a constant load while Vicker's indents penetrate into the sample surface abruptly under the load used. A set of loading and unloading curves (called P-h curves) are shown in Figure 4(c).

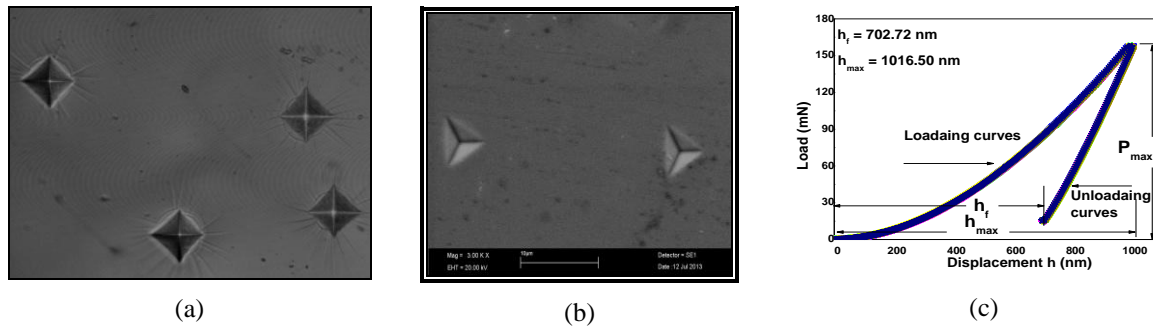


Figure 4 (a). Vicker's (b) and Berkovich indents over the MSRs (c) P-h curves of the alloy.

Penetration depth (displacement) of the indent into the sample is denoted by " $h_f$ " and measured to be 702.7 nm and maximum displacement " $h_{max}$ " is 1016.5 nm. The elastic recovery and percentage elastic recovery of displacement on unloading are two important parameters [27]. The elastic recovery can be determined by the ratio of  $h_f/h_{max}$  and found to be 0.70 while percentage elastic recovery %  $R = ((h_{max}-h_f)/h_{max}) * 100$  % was calculated to be 31 %. These values indicate good mechanical properties at nano scale level. Average nanohardness to elastic modulus ratio H/E was found to be 0.07 and is approximately close to 0.1 indicating that the bonding in amorphous Fe-B-Si alloy is most probably covalent rather than ionic. Covalently bonded materials exhibits a higher H/E than that of a metal; the H/E ratio is about 0.1 for most covalently bonded materials as compared to about 0.002 for face centered cubic (fcc) metals [28]. In some of the P-h curves, pop-in (displacement discontinuities) in loading curves or pop out marks in unloading curves are observed when enlarged many times. The pop-in marks indicate a sudden penetration of the tip of the indent into the sample. The non-uniform penetration is also due to sudden plastic deformation or formation of cracks. Iqbal et al. [4] have reported existence of pop-in/pop-out marks in loading/unloading curves for amorphous steels. The results presented are verified and authentic. The  $Fe_{77.5}Si_{13.3}B_{9.2}$  alloy shows promising thermal and mechanical properties suitable for industrial and commercial applications. The work presented on this alloy will be beneficial for opening new window of applications of Fe-based alloys in paint and textile industries as such alloys are proved to be useful for decolorization of azo dyes (unpublished results). This material will be useful for jewelry applications as well for decolorization of industrial azo dyes. Due to promising mechanical, thermal and magnetic (already published) properties of Fe-B-Si system, we want to use this material in near future for making amorphous transformers (core windings by Fe-B-Si MSRs) and replace Si steel transformers. Work on core windings

has been initiated. Results on decolorization of azo dyes are being submitted. This  $Fe_{77.5}Si_{13.3}B_{9.2}$  and other similar Fe-based amorphous alloys will be used for paint and textile industry, water filtration plants and decolorization of commercial azo dyes.

#### 4. Conclusions

Melt spun ribbons of  $Fe_{77.5}Si_{13.3}B_{9.2}$  alloy were prepared and characterized by various techniques. XRD results showed that as cast MSRs are fully amorphous. DSC results show multistage crystallization. The alloy shows wide supercooled liquid region of 60 K and very high activation energy of 397 kJ/mol indicating good thermal stability and high resistance against crystallization. Vicker's hardness, nanohardness and elastic modulus of the alloy was found to be 760, 11.2 GPa and 170 GPa respectively. The alloy shows unique set of properties due to enhanced closed packed structure by introducing smaller size atoms of B in between Fe and Si atoms in amorphous matrix of Fe. It is expected that the present work on Fe-Si-B alloy will be useful for commercial and industrial applications.

#### Acknowledgements

The first author Muhammad Iqbal gratefully acknowledges the provision of the travel grant and financial support provided by TWAS and CAS, Beijing, China. I am grateful to all group members of MSG, PD PINSTECH and all group fellows of BMG group IOP, Beijing China. Many thanks to Prof. D.Q. Zhao, P. Wen, Dingda Wei, D.P. Wang, Ma Jiang, Bo Huang, Gao, Cui, S.T. Liu, Jiao and Z.G. Zhu for technical help and support. Special thanks to Prof. C. Dong, Y.M. Wang and J.B. Qiang of DUT, Dalian, China for the excellent co-operation. I gratefully acknowledge the invitation and technical support provided by Prof. Z.Q. Hu, J.Z. Zhao and H.F. Zhang for inviting me at IMR, Shenyang, China and to support technically. Thanks to PAEC Pakistan for permission and support to do this work at China.

**References**

- [1] A. Inoue, Proc. Jpn. Acad. **81** B, Ser. B (2005) pp. 156-171.
- [2] A. Inoue, Review: Bulk glassy and nonequilibrium crystalline alloys by stabilization of supercooled liquid: fabrication, functional properties and applications (part 2), in Proc. Jpn. Acad. **81** B, Ser. B (2005) 171-188.
- [3] H. Chiriac and N. Lupu, Mater. Sci. Eng. A **375-377** (2004) 255.
- [4] M. Iqbal, J.I. Akhter, H.F. Zhang and Z.Q. Hu, J. Non-Cryst. Solids **354** (2008) 3284.
- [5] M. Iqbal, J.I. Akhter, H.F. Zhang and Z.Q. Hu, J. Non-Cryst. Solids **354** (2008) 5363.
- [6] C.Q. Zhang, H.F. Zhang, M.Q. Lv and Z.Q. Hu, J. Non-Cryst. Solid **356** (2010) 1703.
- [7] C.Q. Zhang, Z.W. Zhu, H.F. Zhang and Z.Q. Hu, J. Environ. Sci. **24** (2012)1021.
- [8] C.Q. Zhang, Z.W. Zhu, H.F. Zhang and Z.Q. Hu, J. Non-Cryst. Solid **358** (2012) 61.
- [9] Y. Okazaki, J. Magn. Mater. **160** (1996) 217.
- [10] A. Basak, A.J. Moses and M.R. Yasin, J. Magn. Mater. **160** (1996) 210.
- [11] Y.B. Kim, D.H. Jang, H.K. Seok and K.Y. Kim, Mater. Sci. Engg. A **449-451** (2007) 389.
- [12] K. Inagaki, M. Kuwabara, K. Sato, K. Fukui, S. Nakajima and D. Azuma, Hitachi Review **60** (2011) 250.
- [13] N. Banerji, U.C. Johri, V. N. Kulkarni and R.M. Singru, J. Mater. Sci. **30** (1995) 417.
- [14] J.I. Akhter, M. Iqbal, M. Siddique, M. Ahmad, M.A. Haq, M.A. Shaikh and Z.Q. Hu, J. Mater. Sci. Technol. **25** (2009) 48.
- [15] J.I. Akhter, M.A. Shaikh, M. Siddique, M. Ahmad, M. Iqbal and Z.Q. Hu, J. Phys. D: Appl. Phys. **35** (2002) 503.
- [16] C.Q. Zhang, Z.H. Zhang, Z. Qi, Y.X. Qi, J.Y. Zhang and X.F. Bian, J. Non-Cryst. Solid **354** (2008) 3812.
- [17] Z.P. Lu, H. Bei and C. T. Liu, Intermetallics **15** (2007) 618.
- [18] Q.J. Chen, J. Shen, D.L. Zhang, H.B. Fan, J. F. Sun and D.G. McCartney, Mater. Sci. Eng. A **433** (2006) 155.
- [19] Z.Z. Yuan, S.L. Bao, Y. Lu, D.P. Zhang and L. Yao, J. Alloy. Compd. **459** (2008) 251.
- [20] Z.L. Long, G. Xie, H. Wei, J. Peng, P. Zhang and A. Inoue, Mater. Sci. Eng. A **509** (2009) 23.
- [21] A. Hruby, Czech. J. Phys. B **22** (1972) 1187.
- [22] M. Saad and M. Poulain, Mater. Sci. Forum **19** (1987) 11.
- [23] Y. Li, J. Mater. Sci. Technol. **15** (1999) 97.
- [24] M.L.F. Nascimento, L.A. Souza, E.B. Ferreira and E.D. Zanotto, J. Non-Cryst. Solids **351** (2005) 3296.
- [25] G.C. Lavorato, G. Fiore, P. Tiberto, M. Baricco, H. Sirkin and J.A. Moya, J. Alloy. Compd. **536S** (2012) S319.
- [26] H.E. Kissinger, Anal. Chem. **29** (1957)1702.
- [27] A. Bolshakov and G.M. Pharr, J. Mater. Res. **13** (1998) 1049.
- [28] J.G. Wang, B.W. Choi, T.G. Nieh and C.T. Liu, J. Mater. Res. **15** (2000) 798.